Unraveling the strain state of GaN down to single nanowires

Thomas Auzelle,[1,2] Zhihua Fang,[1,2] Xavier Biquard,[3,4] Hervé Roussel,[5,6] Edith Bellet-Amalric,[1,2] Ana Cros,[7] and Bruno Daudin[1,2]

[1)] *Université Grenoble Alpes, INAC-PHELIQS, NPSC, F-38054 Grenoble, France*
[2)] *CEA, INAC-PHELIQS, NPSC, F-38054 Grenoble, France*
[3)] *Université Grenoble Alpes, INAC-PHELIQS, NRS, F-38054 Grenoble, France*
[4)] *CEA/UJF-Grenoble1, INAC-PHELIQS, NRS, F-38054 Grenoble, France*
[5)] *Université Grenoble Alpes, INAC-PHELIQS, NM, F-38054 Grenoble, France*
[6)] *LMGP, Minatec, Grenoble, France*
[7)] *Materials Science Institute, University of Valencia, ICMUV, P.O. Box 22085, E46071, Valencia, Spain*

(Dated: 9 August 2016)

GaN nanowires (NWs) grown by molecular beam epitaxy are usually assumed free of strain in spite of different individual luminescence signatures. To ascertain this usual assumption, the c/a of a GaN NW assembly has been characterized using both X-ray diffraction and Raman spectroscopy, with scaling the measurement down to the single NW. Free-standing single NWs have been observed free of strain – defined as $[c/a-(c/a)_o]/(c/a)_o$ – within the experimental accuracy amounting to 1.25×10^{-4}. However, in the general case, a significant portion of the NWs are coalesced, generating a tensile strain that can be partly released by detaching the NWs from their substrates. It is concluded that at the scale of the single NW, the free surface and the residual doping are not generating a significant strain and only coalescence does.

I. INTRODUCTION

In virtue of the principle of Saint-Venant, nanowires are usually claimed to be strain free, *i.e.* exhibit the same lattice constant than their bulk counterpart. This behavior is assumed in calculations of NW heterostructures[1–3] and fits with experimental reports emphasizing a vanishing of the epitaxial strain away from the NW anchoring site[4–7]. Furthermore, direct lattice parameter measurements based on X-ray diffraction have been performed on self-organized GaN NWs assemblies grown by molecular beam epitaxy (MBE) and emphasize an *average* absence of strain[4,8,9]. However, Jenichen *et al.* [8] and Kaganer *et al.* [4] have both highlighted the existence of lattice parameter fluctuations within GaN NWs assemblies, a so-called micro-strain, amounting between 10^{-3} and 10^{-4}. One has to recall that those measurements have been obtained by integrating the X-ray diffraction signal over more than 10^7 NWs at the same time, which questions whether the observed strain fluctuations occurs between and/or within NWs. In those two reports, the authors have assumed *each* single NW free of strain on average and have related the micro-strain to a residual epitaxial strain (amounting to 10^{-3} at the NW basis) and to the partial coalescence of NWs (amounting to 10^{-4}). Their initial assumption mostly relies on the idea that within an assembly all NWs are similar on average, which is now in contradiction to recent publications emphasizing that each single NWs of an assembly can be particularized through a specific set of characteristics (*e.g.* a specific band edge luminescence[10], a specific excitonic lifetime[11], a probability of hosting an inversion domain[12] and net charges in the native oxide capping[13]). Hence, a strain characterization at the single NW scale becomes desirable.

Indirect estimation of the average strain of a small number of GaN NWs ($\sim$ 100 NWs) can be provided by photoluminescence or Raman spectroscopy and usually indicates an average relaxation[8,14]. To scale further down the characterization, Schlager *et al.* [15] have acquired $\mu-$PL spectra on single GaN NWs dispersed on a foreign substrate. However, such process is adding a spurious interaction of the substrate, which, for instance, manifests itself by generating a temperature dependent strain attributed to the different thermal expansion coefficients between the substrate and the NWs[16]. To overcome this issue, Brandt *et al.* [17] have succeeded to acquire $\mu-$PL spectra on single free-standing self-organized GaN NWs, thanks to low density samples. However, to reach this goal the NWs were grown at unusually high temperature, which has been later reported to imply a residual Si-doping[18], likely generating a residual strain[19]. Nevertheless, the authors have observed small fluctuations in the recombination energy of donor-bound-excitons (~ 3 meV), that they have attributed to surface-related effects rather than to residual strain.

Therefore, to ascertain the strain state of single NWs, a direct measurement by X-ray diffraction remains necessary and is in the scope of this work. The strain state of single GaN NWs either free-standing, coalesced or dispersed on a foreign substrate is addressed using both X-ray diffraction and Raman spectroscopy. Free standing NWs were observed free of strain within the experimental resolution only if free of coalescence.

II. EXPERIMENTS

A. NW growth

NWs have been grown by plasma-assisted MBE on a 2 inch Si(111) substrate. De-oxidation of the silicon was

done by *in situ* annealing up to 950 °C and checked by the observation of a clear 7x7 surface reconstruction at 820 °C. GaN NWs have been grown for more than 14 hours with a III/V ratio of 0.4. Due to the heater geometry, the substrate temperature monotonously decreases from its center to its edge. By setting a nominal temperature of 900 °C no growth of GaN occurred in the substrate center, whereas a fully coalesced assembly of GaN NWs was obtained close to substrate edge with a continuous transition in-between those two extremes[20]. A SEM overview of the NWs as function of d, the distance from the substrate edge, is given in Figure 1a. In addition, to study the impact of the substrate on the NW strain, a few NWs were detached and have been dispersed on different substrates.

B. Coalescence state of free-standing NWs

It can be empirically stated that the coalescence state of NWs increases while decreasing d, *i.e.* from the substrate center to the edge. Therefore, in agreement with the graph of Figure 1b, the NW state of coalescence is correlated to the NW surface filling factor and is anti-correlated to the NW density. When the NW surface filling factor reaches values above 90%, the coalescence state of the NWs is so high that the denomination "compact layer" will be used next. To go further and estimate an absolute degree of coalescence of a NW assembly, Brandt *et al.* [21] have proposed the calculations of two criteria based on the NW top facet geometry. However, as shown in Figure 1c, for the sample under scrutiny the two calculated degrees of coalescence do not monotonously evolve as function of d and both peak at $d \simeq 10$ mm, suggesting a small decrease of the NW coalescence state from $d = 9$ mm to $d = 6$ mm. This feature is considered as an inherent artifact of the two calculated criteria which are only taking into consideration the NW top facet. Indeed, NWs in $d = 6 \sim 9$ mm are largely coalesced at their bottom but feature a rather circular top facet which is associated with an absence of coalescence for those two criteria. Hence, it impedes their solely use for an absolute estimation of the NW degree of coalescence and it becomes advisable to couple them with conventional criteria such as NW surface filling factor, NW density or NW diameter as recently proposed by Kaganer *et al.* [22].

C. Strain measurement

The average strain of the NW assembly has been measured first by laboratory X-ray diffraction using a Seifert XRD 30003 PTS-HR system equipped with a parabolically bend multilayer, a four circles Eulerian Cradle for sample and detector positioning and a 2-fold Ge(220) monochromator. The Cu Kα1 radiation ($\lambda = 0.154056$ nm) was used. In order to average over all the NWs which have a large tilt dispersion (up to $\sim 3^o$ in the substrate center), the measurements have been performed using the extended Bond method[23] at two different locations of the sample which exhibit different NW coalescence states. The method consists of measuring the diffraction from several lattice planes (hkl) belonging to the same crystallographic zone. For each asymmetrical reflexion ω scans are performed in grazing incidence and grazing emergence. From the value $\Delta\omega_{hkl-\overline{hkl}}$, one can infer a c/a value for the GaN NWs. The values obtained for several pairs of asymmetric reflections are given in Table I and their average are reported in Figure 5a. For measurements performed at the same location on the substrate, a large dispersion in the obtained c/a values is observed. It is related to the high inhomogeneity of the sample at the scale of the area exposed to the X-ray beam (about 1.2×12 mm^2). Especially, the measurements of the asymmetric pairs imply to switch from a grazing to a normal incidence, hence NWs with different strain states are probed during one acquisition. Nevertheless, a residual tensile strain in the NWs is observed, especially in the fully coalesced area.

Dist. d from edge	Bond measurements				Statistics	
	Asymmetric reflections				Ave.	Std. Dev.
	(±105)	(±106)	(±204)	(±205)		
4 ± 3 mm	1.620	1.619	1.622	1.622	1.621	0.002
9 ± 3 mm	1.623	–	1.625	1.625	1.624	0.001

TABLE I. c/a values measured by X-ray diffraction using the Bond method, at two different locations over the sample and for different couple of asymmetric reflections. c/a standard deviation (Std. Dev.) and average (Ave.) are given for each locations.

In order to scale down the strain measurement, micro-Raman measurements were performed by means of a HORIBA Jobin Yvon Xplora spectrometer equipped with Peltier-cooled charge coupled device detector and the 532 nm line of a laser diode. Spectra from as-grown NWs at different positions of the substrate radius were obtained in backscattering geometry along the NWs axis, $z(-,-)\overline{z}$. A 100x microscope objective was used to focus the excitation laser on the sample and collect the scattered light to the spectrometer, with a laser power density of 10^5 Wcm^{-2} and a spot size not smaller than 1 μm. In order to check the absence of temperature related measurement artifacts and increase measurement statistics, the micro-Raman analysis was also performed in $z(-,-)\overline{z}$ and $x(-,-)\overline{x}$ geometries by using a 50x microscope objective and a Horiba Jobin Yvon iHR320 spectrometer. In this equipment, the focused size of the 532 nm laser spot was increased to around 50 μm by guiding the incident and scattered light through a multimode fiber, reducing the laser power density to 3×10^3 Wcm^{-2}. At last, NWs detached from their substrates and dispersed on highly ordered pyrolitic graphite (HOPG) have

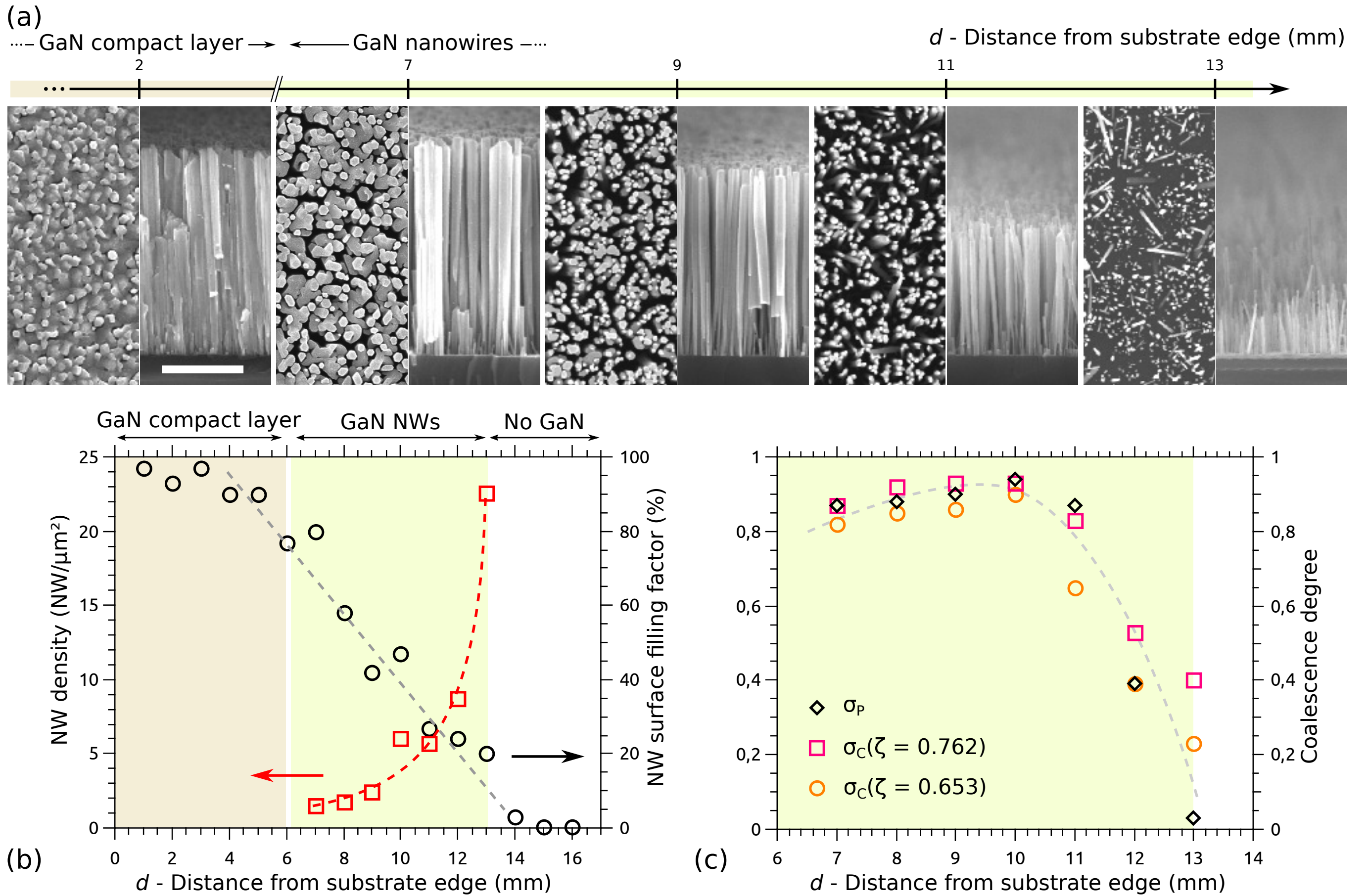

FIG. 1. (a) SEM top and side view of the GaN NW assembly as function of the distance d from the substrate edge – scale bar: 1 μm. (b) NW density and NW surface filling factor as function of the distance d from the substrate edge. (c) Coalescence degree calculated along the two methods proposed in the reference [21] – the gray dotted line is a guide to the eye

been measured by the HORIBA Jobin Yvon Xplora apparatus. In Figure 2a, the Raman spectra acquired on the NW assembly (at $d = 10$ mm) emphasize a peak at ~ 566 cm^{-1}, which is attributed to the E_{2h} optical phonon mode. The wavenumber of the E_{2h} maximum intensity as function of the distance d has been plotted in Figure 2b and exhibits a systematic redshift compared to the value of 567 cm^{-1}, taken here as a reference (it corresponds to the E_{2h} mode in relaxed bulk GaN[24]). This behavior has been checked not to be related to the laser power density neither to the acquisition geometry. In addition, a similar behavior has been already qualitatively reported in reference [14]. Interestingly, once the NWs are detached from their substrate, the E_{2h} value shifts back to the value of the relaxed GaN reference. Using the deformation potentials (α, β) measured by Davydov *et al.* [25] on GaN thin films and the calculated elastic coefficients of GaN, C_{ij}[26], the shift of the E_{2h} peak compared to the bulk relaxed reference, $\Omega_{E_{2h}}$, becomes a function of ϵ_x $(= \epsilon_y)$ and ϵ_z $(= q\epsilon_x)$. Hence, whether assuming a biaxial strain,

$$\sigma_z = 0 \quad \Rightarrow q_{biaxal} = \frac{-2C_{13}}{C_{33}} \tag{1}$$

or an hydrostatic strain,

$$\sigma_x = \sigma_y = \sigma_z \quad \Rightarrow q_{hydro} = \frac{C_{11} + C_{12} - 2C_{13}}{C_{33} - C_{31}} \tag{2}$$

one can extract a value of c/a for the NWs under scrutiny:

$$\frac{c}{a} = \frac{c_0}{a_0}\frac{(1 + q\epsilon_x)}{(1 + \epsilon_x)} \text{ with } \epsilon_x = \frac{\Delta\Omega_{E_{2h}}}{2\alpha + \beta q} \tag{3}$$

The calculated values of c/a are reported in the Figure 5a. In the biaxial approach, a close agreement with the Bond X-ray measurement is obtained in the areas with a large coalescence degree ($d < 9$ mm).

For ultimate strain measurements at the scale of single NWs, X-ray microdiffraction measurements have been performed at the ESRF on the French CRG beamline IF-BM32. A dedicated sub-micronic (ø 300 nm) white beam ($5 - 22$ keV) μLaue diffraction setup has been used to illuminate only a few as-grown NWs and single NWs mechanically dispersed on sapphire and on silica substrates. In the former case, although several NWs are diffracting the X-ray beam, they can still be differentiated from each other thanks to their tilt and twist dispersion, allowing

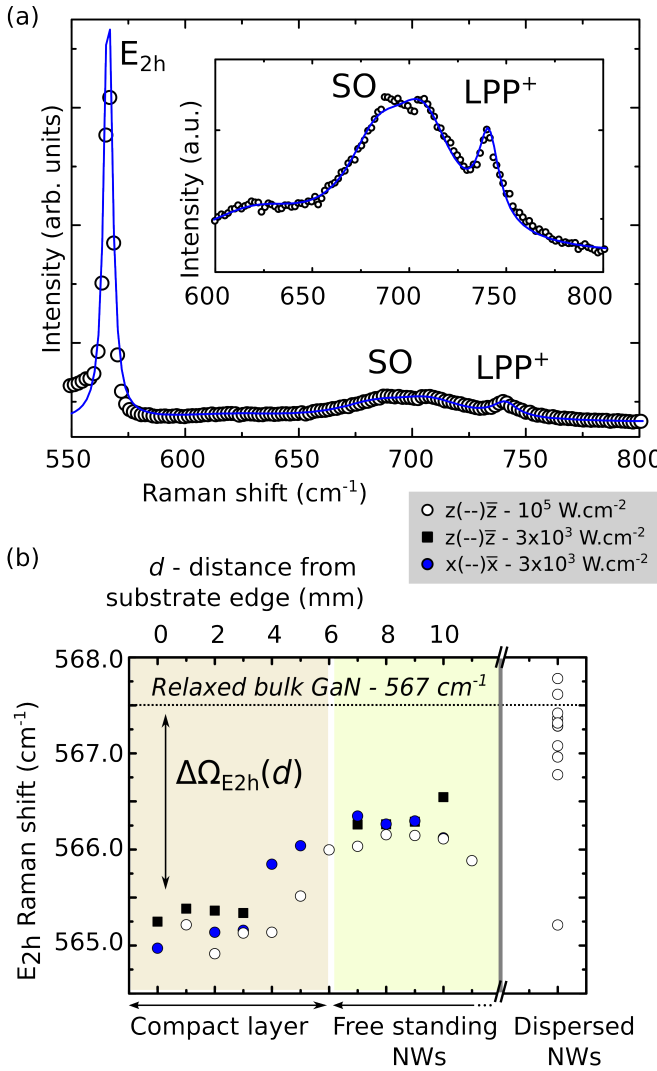

FIG. 2. (a) Raman spectra of GaN NWs acquired at $d =$ 10 mm and fitted (blue curve) by using a model based on the effective dielectric function approximation[27], the inset is a zoom over the LPP+ and LO phonons contributions; (b) wavenumber of the E_{2h} peak measured on NWs attached to the substrate or dispersed on HOPG, acquired using different scattering geometries and illumination intensities.

to associate one set of diffraction peaks to a single NW (see Figure 3b). In the latter case, single NWs are localized first by optical microscopy and then by mapping the fluorescence signal of Ga (see Figure 4b). Next, without the need for sample movement, a large number (> 50) of diffraction peaks for each single NWs are collected on a large area CCD camera, resulting in a micrograph as shown in Figure 3c. Note that in this diffraction configuration only the deviatoric component of the NW strain tensor is measured here (*i.e.* equal deformations in the $\vec{a}$, $\vec{b}$ and $\vec{c}$ directions of the GaN lattice are not visible).

The assembly of peaks are fitted by the Laue spectra of a wurtzite crystal, using the ratio c/a as a unique fitting parameter, thus neglecting possible torsional deformations. Prior to each sample measurement, the exact position of the CCD camera relative to the focal point of the X-ray beam is calibrated by acquiring a Laue spectra on a germanium bulk crystal assumed to be free of strain. In the case of as-grown NWs, 50 spectra acquired on the same NW and on the course of several minutes have provided a set of 50 c/a values having a dispersion of 1.25×10^{-4} which will be considered as the error bar of the measurement (Figure 3d). The c/a values of several single NWs have been measured and reported as function of d on the graphs of Figure 5. Interestingly, two families of NWs could be distinguished from their Laue spectra: NWs having round shape diffraction peaks and NWs having diffraction peaks showing irregular shapes. Measurements of the former always exhibit an absence of strain within the accuracy of the measurement (1.25×10^{-4}) whereas measurements of the latter have always revealed the presence of strain, whether tensile or compressive. Hence, the strain in NWs was never observed to be homogeneous and results in distorted NWs. Note also that because they are wider, the maximum intensity of the irregular diffraction peaks is lower and possibly reaches the noise level, which decreases the sensibility of the Laue technique to distorted NWs.

For NWs detached from their substrate and dispersed on different types of substrates, unexpected small displacements of the NWs under the X-ray beam exposure have been observed. As shown in Figure 4a, the angular position of a NW lying on silica has been recorded through time and emphasizes a steady rotation speed around its c axis of $0.45°.\text{min}^{-1}$. This phenomenon was observed whether NWs were dispersed on silica, silicon, sapphire or germanium but the rotation speed was qualitatively reduced if using more conductive substrates (*e.g.* germanium or silicon). There is no clear mechanism to explain the NW rotation but one can incriminate electronic charging of the NWs (knowing that the X-ray beam easily ionizes Ga and N atoms as testified by the measured fluorescence signal or their luminescence in the visible range) combined with contamination by on-going carbon deposition.

Nevertheless, the c/a values of NWs dispersed on silica and sapphire have been continuously measured during exposure to the X-ray beam, on a time scale of several minutes, as shown in Figure 4d. After several tens of seconds, the measured c/a abruptly shift from ~ 1.626 (*i.e.* the approximate value expected for relaxed NWs) to 1.625 with a dispersion of $\pm 6 \times 10^{-4}$. This behavior will be assigned to the electrical charging of the NWs. Since it corresponds to a measurement artifact, only the c/a values acquired in the very first seconds of the measurement will be further considered. Those c/a values measured on dispersed NWs are reported in the graphs of Figure 5.

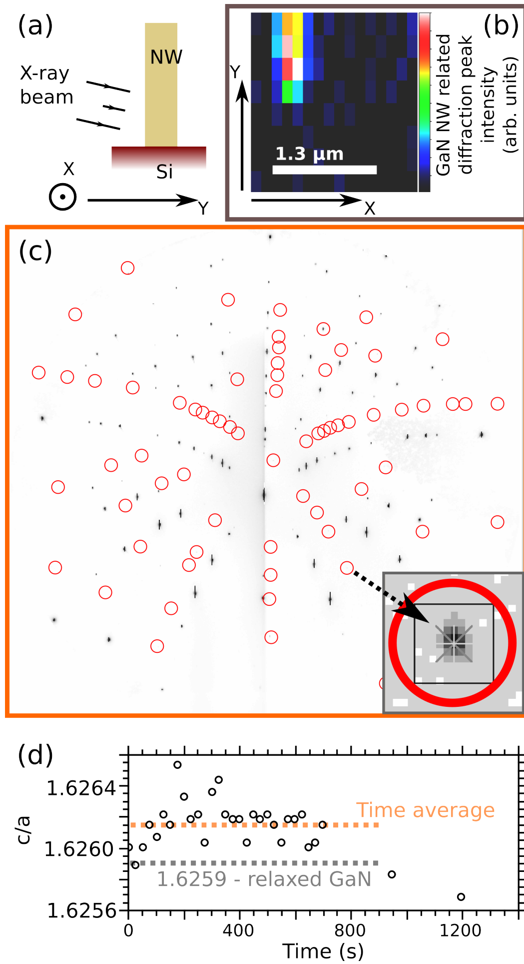

FIG. 3. (a) Schematic of the diffraction geometry. (b) Spatial mapping of a single GaN NW diffraction peak intensity used to precisely locate the NW. The signal is elongated along the Y direction due to the grazing incidence of the X-ray beam. (c) Full Laue spectra acquired on the single NW – the superimposed red circles highlight the diffraction peaks of a single NW, other peaks correspond to the Si substrates – a zoom over one GaN related peak is shown in the inset. (d) Measured c/a of the single NW as function of time.

D. Doping measurements

Because doping could affect the strain of GaN NWs[19], a measurement of the average residual doping of the NWs has been performed. We remind that NWs have been grown without intentional doping but impurities in the growth chamber, etching of the Si substrate surface by Ga[18] or Si diffusion from the substrate[28,29] could account for a residual doping.

Using a similar technique as in reference [19], the density of charge carriers in one dispersed NW has been extracted from transport measurements and amounted to $3 \sim 4 \times 10^{17}$ cm^{-3}.

In addition, the charge carrier density can be estimated from the wavenumber of the phonon-plasmon coupled

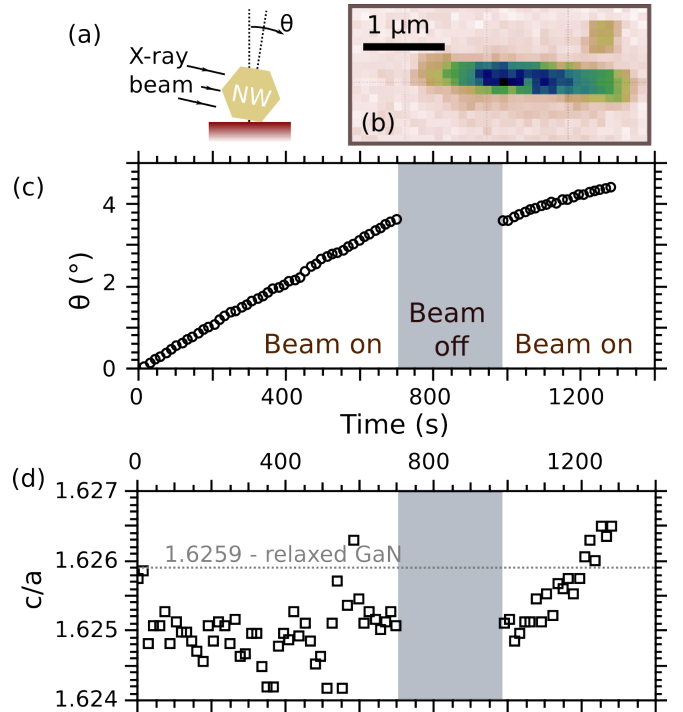

FIG. 4. (a) Schematic of the diffraction geometry, (b) mapping of the Ga fluorescence signal revealing the presence of a 2 μm long bunch of single dispersed NWs, (c) angular position of a dispersed NW on silica as function of time, (d) c/a values measured as function of time.

mode (LPP+ at $\sim$ 741 cm^{-1}), and the surface optical modes (SO at $\sim$ 700 cm^{-1}) both showing up in the Raman spectra (see inset of Figure 2a). Using a model based on the effective dielectric function approximation[27] that takes into account the phonon-plasmon coupling[30], the Raman spectra fitting provides a free carrier density of 2.5×10^{17} cm^{-3} in agreement with the transport measurements.

Hence both measurements indicate a moderate doping of the NWs.

III. DISCUSSION

One uses here a strain defined as:

$$\epsilon_{c/a} = \frac{c/a - c_o/a_o}{c_o/a_o} = \frac{1 + q\epsilon_x}{1 + \epsilon_x} - 1 \quad (4)$$

where c_o/a_o is the GaN strain free value of c/a, taken as 1.6259, according to the statistical analysis of Robins *et al.* [9] performed on several published works concerning NWs, films and bulk GaN. $q = \epsilon_z/\epsilon_x$ and it is assumed that $\epsilon_x = \epsilon_y$.

For the compact layer (NW surface filling factor > 90% as found in $d = 0 \sim 5$ mm), both the Raman spectroscopy and the Bond X-ray diffraction indicate $\epsilon_{c/a} \simeq -2.4 \times 10^{-3}$, corresponding to a biaxial tensile strain, *i.e.* $\sigma_z = 0$. Two contributions to this strain can be invoked:

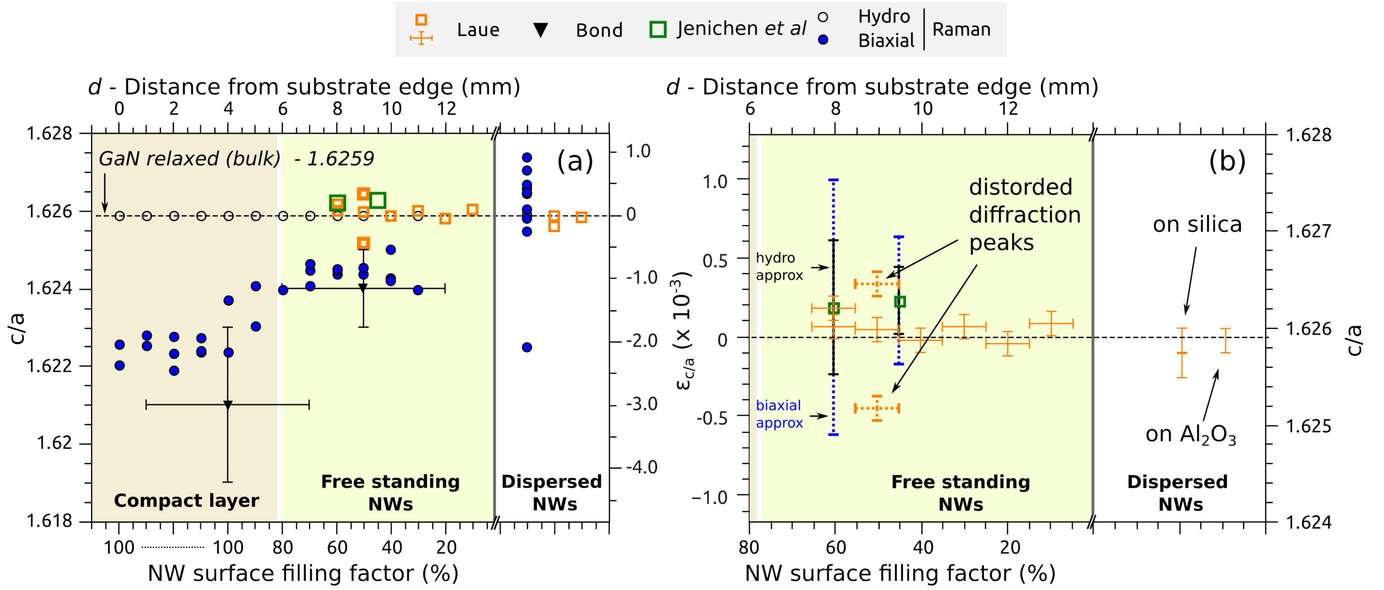

FIG. 5. (a-b) Average c/a values of GaN NWs measured by using Bond X-ray diffraction measurements, c/a estimated from the E_{2h} phonon mode shift and whether assuming a biaxial or an hydrostatic strain, c/a values of single GaN NWs obtained by Laue diffraction and c/a values published in literature for similar samples (Jenichen *et al.* [8] and Robins *et al.* [9]). In the panel (b), errors bars for Laue diffraction measurements corresponding to the experiment accuracy have been added. The bars around the data set of Jenichen *et al.* [8] correspond to the c/a dispersion observed in their sample, whether considering a biaxial (blue) or an hydrostatic (dark) strain. $\epsilon_{c/a} = \frac{c/a - c_o/a_o}{c_o/a_o}$ where $c_o/a_o = 1.6259$ is assumed to be the relaxed c/a value of GaN[9].

- the difference between the thermal expansion coefficient of GaN and its Si substrate. Indeed, using a constant in-plane expansion coefficient of 5×10^{-6} K^{-1} for GaN[31] and 3.5×10^{-6} K^{-1} for Si[32] over the range 300 ∼ 1000 K, an in-plane deformation of $\epsilon_x \simeq 10^{-3}$ is expected, resulting in a $\epsilon_{c/a} \simeq -1.8 \times 10^{-3}$, which lies in the order of magnitude of the experimental data.

- coalescence of crystallites. Such process has been theoretically reported to generate a biaxial tensile strain[33] related to the energy gain obtained by suppressing free surface. It has been experimentally evidenced by Hugues *et al.* [6] for GaN pillars, resulting in a tensile strain amounting in their case to $\epsilon_x = 10^{-3}$, which lies also in the experimental order of magnitude of our data.

Those two contributions should vanish along with a decrease of the coalescence state, which is observed for $d = 4 \sim 7$ mm both by the Bond X-ray diffraction and the Raman analysis.

For the area having a NW surface filling lower than 20% (*i.e.* $d \geq 12$ mm) the probability of having coalescence between NWs is negligible on the basis of structural imaging performed by SEM (see Figure 1a). There, the probing of single free standing NWs by Laue diffraction gives $\epsilon_{c/a} < 1.25 \times 10^{-4}$, which corresponds to the experimental precision. It means that the residual doping of the NWs (estimated lower than 10^{18} at.cm^{-3} from the free carrier measurements) and the presence of the free surface (including oxide and possible surface defects) do not generate a strain above 1.25×10^{-4} for the whole NW.

While the NW surface filling factor increases from 20 to 80% (*i.e.* from $d = 8$ mm to $d = 11$ mm), the probability of having coalescence between two single NWs increases and is correlated with the appearance of a few strained NWs according to the Laue technique. Actually, two coexisting populations of NWs are clearly put in evidence by the Laue technique: one of NWs free of strain and rather homogeneous as indicated by the round shape diffraction peaks, and one of strained NWs which are highly inhomogeneous as indicated by the distorted diffraction peaks. Hence, the first population is assigned to uncoalesced free standing NWs whereas the second one is attributed to coalesced NWs. In contrast, in the same substrate area, both the Bond X-ray technique and the Raman spectroscopy indicate an average tensile strain for the NW assembly. This behavior is qualitatively different from the one described by the Laue technique and is assigned to a scaling effect. Indeed, the Laue technique provides insight on a limited number of NWs and the data processing has usually favored the study of unstrained NWs as they exhibit intense and circular diffraction peaks. In contrast, the Raman spectroscopy and the Bond X-ray technique provide an average measurement of *all* the NWs, including the coalesced ones. Therefore, the residual tensile strain observed by those two tech-

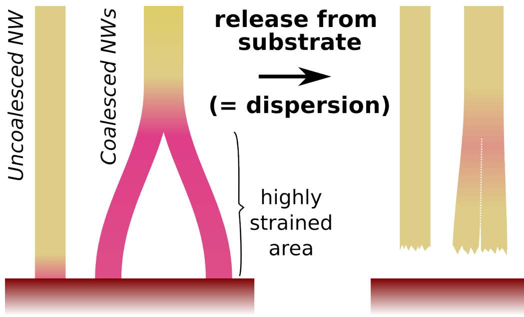

FIG. 6. Schematic of the expected strain release following NW dispersion. The strained sections of the NWs are highlighted in red.

niques is attributed to NW coalescence.

Once detached from the substrate and dispersed, NWs were observed on average free of strain both by the Laue technique and the Raman spectroscopy. It suggests that the epitaxial relationship between the substrate and the NWs has a large contribution in the coalescence induced strain. Such phenomenon could be ascribed to NW coalescence through the bundling mechanism described by Kaganer *et al.* [22], for which detaching NWs would release a significant part of the strain, as sketched in Figure 6.

For comparison purpose, the strain state of the two GaN NW assemblies grown on Si and measured by Jenichen *et al.* [8] has been superimposed on the graphs of Figure 5. Both their NW surface filling factor and coalescence degree have been extracted from the SEM top view images provided in their publication. Note that the correspondence between the two parameters was in agreement with the one measured on our sample and plotted in Figure 1. The authors have observed an increasing dispersion in ϵ_z along with the coalescence. Using either the biaxial or the hydrostatic approximation, this dispersion has been translated into a c/a dispersion and is displayed in Figure 5b as errors bars. Their amplitudes are found to be in agreement with the data set obtained with the Laue technique but slightly disagrees with the one of Raman spectroscopy and Bond X-ray technique. The discrepancy can be tentatively assigned to a different measurement configuration as the authors have used $\theta/2\theta$ scans normal to the substrate surface to extract the average c lattice constant of the GaN NWs. Indeed, by doing so, they have probed only the NWs having a negligible tilt, hence they might have non-intentionally selected NWs free of coalescence.

IV. CONCLUSION

Raman spectroscopy and X-ray diffraction have been used in order to measure the strain state of a GaN NW assembly grown on Si from large scale down to the single NW. A large tensile strain ($\epsilon_{c/a} = -2.4 \times 10^{-3}$) has been observed for fully coalesced NWs and assigned to the different thermal expansion between the Si substrate and the NWs as well as to the result of coalescence itself. For NW assemblies having a filling factor below 20%, NWs were individually observed free of strain within the accuracy of the experimental setup ($i.e.$ $\epsilon_{c/a} < 1.25 \times 10^{-4}$) whereas for NW assemblies having a filling factor between 20 and 80%, a part of the NW assembly has coalesced and exhibit an average tensile strain. Interestingly, a significant part of this strain can be released by detaching the NWs from their substrate. It is concluded that at the scale of the single NW, the free surface and residual doping are not generating a significant strain and only coalescence does. Hence, in the light of this work, the reported fluctuations from single NW to single NW of the excitonic lifetime[11] and D^oX recombination energy[10] cannot be attributed to strain fluctuations between NWs.

[1] F. Glas, Phys. Rev. B **74**, 121302 (2006).
[2] E. Ertekin, P. A. Greaney, D. C. Chrzan, and T. D. Sands, Journal of Applied Physics **97**, 114325 (2005).
[3] X. Zhang, V. G. Dubrovskii, N. V. Sibirev, and X. Ren, Crystal Growth & Design **11**, 5441 (2011), http://dx.doi.org/10.1021/cg201029x.
[4] V. M. Kaganer, B. Jenichen, O. Brandt, S. Fernández-Garrido, P. Dogan, L. Geelhaar, and H. Riechert, Phys. Rev. B **86**, 115325 (2012).
[5] W. J. Tseng, M. Gonzalez, L. Dillemans, K. Cheng, S. J. Jiang, P. M. Vereecken, G. Borghs, and R. R. Lieten, Applied Physics Letters **101**, 253102 (2012).
[6] M. Hugues, P. A. Shields, F. Sacconi, M. Mexis, M. Auf der Maur, M. Cooke, M. Dineen, A. Di Carlo, D. W. E. Allsopp, and J. Zúñiga-Pérez, Journal of Applied Physics **114**, 084307 (2013).
[7] A. Biermanns, S. Breuer, A. Davydok, L. Geelhaar, and U. Pietsch, Journal of Applied Crystallography **45**, 239 (2012).
[8] B. Jenichen, O. Brandt, C. Pfüller, P. Dogan, M. Knelangen, and A. Trampert, Nanotechnology **22**, 295714 (2011).
[9] L. H. Robins, K. A. Bertness, J. M. Barker, N. A. Sanford, and J. B. Schlager, Journal of Applied Physics **101**, 113505 (2007).
[10] C. Pfüller, O. Brandt, T. Flissikowski, C. Chéze, L. Geelhaar, H. Grahn, and H. Riechert, Nano Research **3**, 881 (2010).
[11] A. Gorgis, T. Flissikowski, O. Brandt, C. Chèze, L. Geelhaar, H. Riechert, and H. T. Grahn, Phys. Rev. B **86**, 041302 (2012).
[12] T. Auzelle, B. Haas, A. Minj, C. Bougerol, J.-L. Rouviére, A. Cros, J. Colchero, and B. Daudin, Journal of Applied Physics **117**, 245303 (2015).
[13] A. Minj, A. Cros, N. Garro, J. Colchero, T. Auzelle, and B. Daudin, Nano Letters **15**, 6770 (2015), pMID: 26380860, http://dx.doi.org/10.1021/acs.nanolett.5b02607.
[14] F. Furtmayr, M. Vielemeyer, M. Stutzmann, A. Laufer, B. K. Meyer, and M. Eickhoff, Journal of Applied Physics **104**, 074309 (2008).
[15] J. B. Schlager, K. A. Bertness, P. T. Blanchard, L. H. Robins, A. Roshko, and N. A. Sanford, Journal of Applied Physics **103**, 124309 (2008).
[16] R. Anufriev, N. Chauvin, H. Khmissi, K. Naji, M. Gendry, and C. Bru-Chevallier, Applied Physics Letters **101**, 072101 (2012).
[17] O. Brandt, C. Pfüller, C. Chèze, L. Geelhaar, and H. Riechert, Phys. Rev. B **81**, 045302 (2010).
[18] J. K. Zettler, C. Hauswald, P. Corfdir, M. Musolino, L. Geelhaar, H. Riechert, O. Brandt, and S. Fernández-Garrido, Crystal Growth & Design **0**, null (0), http://dx.doi.org/10.1021/acs.cgd.5b00690.
[19] Z. Fang, E. Robin, E. Rozas-Jiménez, A. Cros, F. Donatini, N. Mollard, J. Pernot, and B. Daudin,

Nano Letters **15**, 6794 (2015), pMID: 26426262, http://dx.doi.org/10.1021/acs.nanolett.5b02634.

[20] R. Mata, K. Hestroffer, J. Budagosky, A. Cros, C. Bougerol, H. Renevier, and B. Daudin, Journal of Crystal Growth **334**, 177 (2011).

[21] O. Brandt, S. Fernández-Garrido, J. K. Zettler, E. Luna, U. Jahn, C. Chèze, and V. M. Kaganer, Crystal Growth & Design **14**, 2246 (2014), http://dx.doi.org/10.1021/cg401838q.

[22] V. M. Kaganer, S. Fernández-Garrido, P. Dogan, K. K. Sabelfeld, and O. Brandt, Nano Letters **16**, 3717 (2016), pMID: 27168127, http://dx.doi.org/10.1021/acs.nanolett.6b01044.

[23] W. L. Bond, Acta crystallographica Section A: foundations of crystallography **13**, 814 (1960).

[24] P. Perlin, C. Jauberthie-Carillon, J. P. Itie, A. San Miguel, I. Grzegory, and A. Polian, Phys. Rev. B **45**, 83 (1992).

[25] V. Y. Davydov, N. S. Averkiev, I. N. Goncharuk, D. K. Nelson, I. P. Nikitina, A. S. Polkovnikov, A. N. Smirnov, M. A. Jacobson, and O. K. Semchinova, Journal of Applied Physics **82** (1997).

[26] K. Sarasamak, S. Limpijumnong, and W. R. L. Lambrecht, Phys. Rev. B **82**, 035201 (2010).

[27] A. Cros, J. Wang, F. Demangeot, R. Péchou, and B. Daudin, Japanese Journal of Applied Physics **52**, 08JL01 (2013).

[28] F. Furtmayr, M. Vielemeyer, M. Stutzmann, J. Arbiol, S. Estradé, F. Peirò, J. R. Morante, and M. Eickhoff, Journal of Applied Physics **104**, 034309 (2008).

[29] M. Schäfer, M. Günther, C. Länger, J. Müßener, M. Feneberg, P. Uredat, M. T. Elm, P. Hille, J. Schörmann, J. Teubert, T. Henning, P. J. Klar, and M. Eickhoff, Nanotechnology **26**, 135704 (2015).

[30] D. T. Hon, W. L. Faust, W. G. Spitzer, and P. F. Williams, Phys. Rev. Lett. **25**, 1184 (1970).

[31] C. Roder, S. Einfeldt, S. Figge, and D. Hommel, Phys. Rev. B **72**, 085218 (2005).

[32] H. Watanabe, N. Yamada, and M. Okaji, International Journal of Thermophysics **25**, 221 (2004).

[33] W. D. Nix and B. M. Clemens, Journal of Materials Research **14**, 3467 (1999).